A note on oblique water entry

M.R. Moore, S.D. Howison, J.R. Ockendon and J.M. Oliver
Mathematical Institute, University of Oxford, 24-29 St. Giles', Oxford, OX1 3LB, UK

Abstract. A minor error in Howison, Ockendon & Oliver (J. Eng. Math. 48:321–337, 2004) obscured the fact that the points at which the free surface turns over in the solution of the Wagner model for the oblique impact of a two-dimensional body are directly related to the turnover points in the equivalent normal impact problem. This note corrects some of the earlier results given in Howison, Ockendon & Oliver (2004) and discusses the implications for the applicability of the Wagner model.

1. Introduction

Water impact problems have important applications in areas ranging from the shipbuilding industry to ink-jet printing. The simplest model for the entry of a solid into a liquid half-space has a long history going back to [11]. One aspect that is the subject of much current research is that of oblique entry.

There is a wealth of literature regarding the constant velocity oblique water-entry of a rigid wedge, for which there is a similarity solution. This scenario is considered in, for example, [1, 2, 3]. For a review of these and others see [10] and the references within. The small-time oblique water-entry of a parabola is considered in [4].

This note looks at more general impactors and, in particular, is concerned with phenomena that can occur when the impact is nearly tangential. Our approach is based on the analysis given in [7], who use the ideas of [11] and the method of matched asymptotic expansions to model general geometries. We will find that the correction of an error made in [7] in the specific example of oblique wedge impact leads to a surprising observation, which applies not only in that example, but also for more general cases. We note how a transformation of the leading-order problem allows us to readily write down the solution and describe the results of this observation on the pressure on the impactor and the splash jets.

Section 2 of [7] describes the dimensionless Wagner model for the oblique impact of a rigid two-dimensional body into an ideal, incompressible liquid half-space beneath an initially horizontal free surface. We start from the dimensional model, in which the liquid lies in the lower half-space $y^* < 0$, where (x^*, y^*) are Cartesian coordinates with origin at the point of impact, which is taken to begin at time $t^* = 0$.


© 2012 *Kluwer Academic Publishers. Printed in the Netherlands.*

Here and hereafter an asterisk indicates a dimensional variable. The body profile is f and its position is given by

$$\frac{y^*}{L} = f\left(\frac{\varepsilon x^*}{L} - \frac{Ut^*}{T}\right) - s\left(\frac{t^*}{T}\right),$$

where Ls is a typical penetration depth; ε is a typical 'deadrise' angle between the tangent to the impactor and the undisturbed free surface; T is a typical impact timescale, so that L/T is a typical normal impact speed; and $UL/\varepsilon T$ is a typical tangential impact speed, so that U/ϵ is the dimensionless ratio of the tangential to the normal impact speeds. We assume that $f(0) = 0$ and f increases as $|x|$ increases. For example, for a parabola whose radius of curvature at the origin is R and whose centre of curvature lies above its minimum, we set $f(x) = x^2/(2R)$, with $\varepsilon = \sqrt{L/R}$. We consider the distinguished limit examined in [7] in which $U = O(1)$ as $\varepsilon \to 0$, so that the angle of attack of the impactor to the undisturbed free surface is comparable to the deadrise angle.

After scaling distances (x^*, y^*), time t^*, the free surface elevation h^*, the velocity potential $\phi^*$and the pressure p^* with L/ε, T, L, $L^2/\varepsilon T$ and $\rho L^2/\varepsilon T^2$, respectively, where ρ is the liquid density, the dimensionless body profile becomes

$$y = \varepsilon\left(f(x - Ut) - s(t)\right)$$

and we obtain, as described in, for example, [9], the mixed boundary value problem for the velocity potential $\phi(x, y, t)$ and free surface $y = \varepsilon h(x, t)$ shown in Figure 1. The two turnover points (where $\partial h/\partial x$ is infinite) are $x = d_\pm(t), y = 0$ to lowest order.

We will now describe the surprising consequences of the fact the 3/4 in the coefficient of the square-root term in (6) in §2.2.1 of [7] should actually be a 3/2. We note that the 3/4 in the coefficient of the arcsine

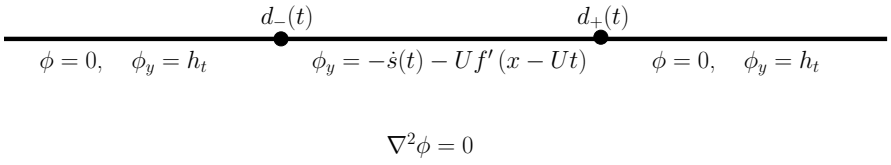

Figure 1. The linearised leading-order outer problem for the velocity potential. The far-field conditions are given by $\phi(x, y, t) = O(1/r)$ as $r^2 = x^2 + y^2 \to \infty$ and $h(x, t) \to 0$ as $|x| \to \infty$. The initial conditions are given by $h(x, 0) = 0$, and $d_\pm(0) = 0$. The velocity potential has square-root behaviour at the turnover points $x = d_\pm(t)$. The problem is closed by the Wagner conditions holding at each free point, namely $h(d_\pm(t), t) = f(d_\pm(t) - Ut) - s(t)$.

term remains correct. Even though this equation was written down for the special case of wedge impact, our remarks will apply to more general impactors. We will also highlight the resulting corrections to the leading-order behaviour of the free points, free surface and pressure on the impactor.

2. Location of the turnover points for wedge impacts

If we define the displacement potential by

$$\Psi(x,y,t) = -\int_0^t \phi(x,y,\tau)\mathrm{d}\tau,$$

the mixed boundary value problem becomes that displayed in Figure 2. The important thing to note here is that this problem contains no time derivatives and that Ψ, unlike ϕ, has bounded gradient at the turnover points. The solution of the resulting Riemann-Hilbert problem of index -1 is given by (3) in [7], with consistency conditions (4).

We consider the case of symmetric wedge impact, for which $f(x) = |x|$, with $s(t) = t$, in which case the turnover points can be written as $d_\pm = a_\pm t$. Correcting 3/4 to 3/2 in the coefficient of the square-root term in (6) of [7], we make the change of variable

$$a_\pm \mapsto U \pm a_\pm,$$

in the resulting equations, so that, upon defining $q_1 = a_+ + a_-$ and $q_2 = a_+ - a_-$, we can reduce the problem to finding q_1 and q_2 such that

$$q_2 \arcsin\left(\frac{q_2}{q_1}\right) = \pi - \sqrt{q_1^2 - q_2^2}, \quad \pi q_1^2 = (q_1^2 - q_2^2)^{3/2}. \tag{1}$$

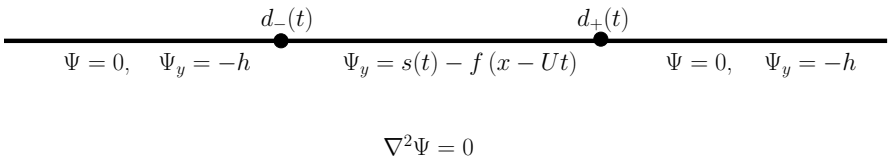

. The displacement potential has (3/2)-power behaviour at the turnover points $x = d_\pm(t)$.

Figure 2. The linearised leading-order outer problem for the displacement potential. The far-field conditions are given by $\Psi(x,y,t) = O(1/r)$ as $r^2 = x^2 + y^2 \to \infty$ and $h(x,t) \to 0$ as $|x| \to \infty$. The initial condition is given by $d_\pm(0) = 0$

Assuming that the free surface does not separate from the wedge apex and that the turnover points are advancing, we must force $d_- < Ut < d_+$, *i.e.* $-q_1 < q_2 < q_1$ and $q_1 > 0$. It is then possible to show by elementary methods that the unique solution to (1) is given by $q_1 = \pi$, $q_2 = 0$. Thus the turnover points for an obliquely impacting wedge are given by $d_\pm = (U \pm \pi/2)t$.

This means that the critical tangential impact speed, U^*, at which the model breaks down in the vicinity of the trailing turnover point, is in fact $U^* = \pi/2$ rather than 0.4853 as given in [7]. At this critical value, the trailing turnover point stops advancing, leading to a local instability to disturbances out of the (x, y)-plane as described in [8].

The correct form of the turnover points gives that, surprisingly, the leading-order outer free surface in the oblique wedge entry problem is still symmetric about the apex of the wedge, $x = Ut$, at leading order, even though the wedge is moving rapidly horizontally.

To see why the symmetry persists and to extend our analysis to more general profiles, we note that under the change of variables

$$d_\pm \mapsto Ut + d_\pm, \quad z \mapsto Ut + z, \quad \zeta \mapsto Ut + \zeta$$

where $z = x + iy$, equation (3) in [7] reduces to

$$\Psi_x - \mathrm{i}\Psi_y = \frac{\mathrm{i}\sqrt{(z - d_+)(z - d_-)}}{\pi} \int_{d_-}^{d_+} \frac{s(t) - f(\zeta)}{\sqrt{(d_+ - \zeta)(\zeta - d_-)}} \frac{d\zeta}{(\zeta - z)}, \quad (2)$$

with the consistency conditions

$$\int_{d_-}^{d_+} \frac{(s(t) - f(\zeta))\,\zeta^j}{\sqrt{(d_+ - \zeta)(\zeta - d_-)}} d\zeta = 0 \quad (3)$$

for $j = 0, 1$.

These are exactly the form of the solution to the corresponding normal impact problem for the body $y = f(x) - s(t)$. Hence, if the normal impact problem has a solution, say with turnover points $d_\pm(t)$, leading-order outer free surface $h(x, t)$ and leading-order displacement potential $\Psi(x, y, t)$, then $d_\pm(t) + Ut$ are the turnover points, $h(x - Ut, t)$ is the leading-order outer free surface and $\Psi(x - Ut, y, t)$ is the leading-order displacement potential for the corresponding oblique impact. In the particular example of a symmetric body profile, the turnover points, displacement potential and free surface are symmetric about the minimum of the impactor, although we note that the velocity potential and pressure are not. We note that this is in agreement with the prediction in [4] that the leading-order displacement potential and turnover points in the oblique impact of a parabola at small times are unaffected by the oblique component of impact velocity.

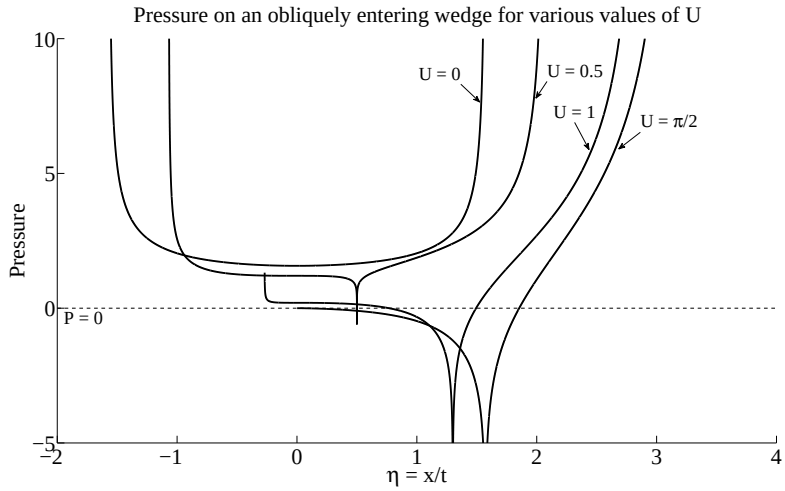

Figure 3. The pressure (in similarity form) on the contact set for a wedge-shaped impactor for various values of U. The wedge apex is at $\eta = U$. The pressure about the apex is asymmetric; as we increase U up to the critical velocity $U = \pi/2$ where $d_- = 0$, the pressure at d_- decreases to zero. The pressure is always negative and infinite at the moving apex, but is non-singular when $U = 0$.

These results generalise to an arbitrary oblique impact component of velocity, say a body profile of the form $y = f(x - X(t)) - s(t)$.

3. Implications of the corrected theory

For the example of wedge entry with $s(t) = t$, the above points imply that Figures 4a-c in [7] are incorrect. Figures 4a-b should both indicate the symmetry; the former plot of the turnover points as a function of U should be the straight lines $x = (U \pm \pi/2)t$ and the latter should depict a free surface profile symmetric about the wedge apex, obtained by translating the normal impact free surface by Ut in the x-direction.

The corrected pressure plot becomes more interesting. The pressure is given by $p = -\phi_t = \Psi_{tt}$. Given the symmetry in the problem, we can evaluate (2) on the impactor, integrate, return to the original coordinates and then twice differentiate with respect to t to explicitly calculate an expression for $p(x,t) = P(\eta)$ where $\eta = x/t$:

$$P = \frac{(\pi/2)^2 - U^2 + 2U\eta}{\sqrt{(\pi/2)^2 - (\eta - U)^2}} + \frac{2U^2}{\pi} \log \left| \frac{\pi/2 - \sqrt{(\pi/2)^2 - (\eta - U)^2}}{\eta - U} \right|. \quad (4)$$

We plot this in Figure 3 for various values of U. The pressure becomes negative and infinite at the apex as expected. Although this negative pressure persists for all $U > 0$, as we increase U, the region of negative pressure grows, particularly on the trailing side of the wedge. At breakdown, we have $U = \pi/2$ and the point of zero pressure on the trailing side coincides with the turnover point. We can verify this by noting the expansion of the pressure on the body near the trailing turnover point is given by

$$P(\eta) = \frac{(U - \pi/2)^2}{\sqrt{\pi}\sqrt{\eta - (U - \pi/2)}} + O\left(\sqrt{\eta - (U - \pi/2)}\right),$$

as $\eta - (U - \pi/2) \downarrow 0$. Hence, the coefficient of the inverse square-root singularity vanishes when $U = \pi/2$. Naturally, this also applies to the inverse square-root singularity in the leading-order outer velocity.

The presence of a region of negative pressure on the wedge raises the possibility of cavitation occurring prior to breakdown. It is possible that a patch cavity forms on the impactor in this region of negative pressure. The dynamics of such cavities are discussed in [5, 6]. Our analysis has implicitly assumed that this does not happen, and also does not affect the breakdown caused by the trailing turnover point no longer advancing.

The breakdown near the trailing edge as we approach the critical velocity has implications for the splash jet there. The splash jet forming at each turnover point emanates from a jet-root region near these points, which are described by Helmholtz flows, as discussed in [8]. In local coordinates moving with the body, the flow in the splash jets is governed by the zero-gravity shallow-water equations for the jet thickness $\tilde{h}$ and tangential velocity component $\tilde{u}$, as described in [8]. These need to satisfy boundary data at the leading and trailing turnover points each one of which is modelled in [9] by

$$\tilde{h} = \frac{\pi}{16}\frac{\mathcal{S}^2}{\mathcal{U}^2}, \quad \tilde{u} = 2\mathcal{U}, \tag{5}$$

where $\mathcal{S}$ is the coefficient of the square root in the leading-order outer velocity potential as we near the respective turnover points and $\mathcal{U}$ is their speed. The coefficient of the square root in the leading-order outer velocity potential can be calculated from a time differentiation of (2). The factor of 2 in (5) arises from the fact that the jet-root region moves with speed $\mathcal{U}$, in addition to the asymptotic value of the fluid velocity in the jet in the Helmholtz flow, as discussed in [8].

It is simple to show that the leading and trailing splash jets are not symmetric and that the length of the trailing jet is given by $(\pi/2 -$

$U)t$, which vanishes as we approach the critical velocity. The maximum thickness of the trailing splash jet is found at the turnover point and is given by $t/4$. Thus, as we approach the critical forward velocity, the aspect ratio of the maximum width to the length of the jet blows up. This means that our assumption of a long, slender jet breaks down as $U \uparrow \pi/2$. Furthermore, since the characteristics for the zero-gravity shallow-water equations are given by particle paths, at breakdown the characteristics are parallel to the boundary curve and hence the model is no longer valid.

4. Generalisations

It is natural to ask whether we can deduce something similar for a more general symmetric body profile, say $f(x) = |x|^n$ and more general impact speed, say $s(t) \propto t^m$ where $m > 0$ and $n \geq 1$. Given the symmetry of the body we may still seek a solution $d_\pm = Ut \pm d(t)$. Hence, the consistency condition for $j = 1$ in (3) is trivially satisfied, whilst the second consistency condition can be integrated upon making the substitution $\zeta = d(t)\sin\theta$. We find

$$d_\pm = Ut \pm \left(\frac{\pi}{2^n \mathrm{B}((n+1)/2,(n+1)/2)}\right)^{1/n} t^{m/n},$$

where $\mathrm{B}(\cdot,\cdot)$ is the beta function.

Breakdown occurs when the trailing turnover point stops advancing. Thus we can enumerate the following cases:

- for $m < n$, this happens after a finite time when

$$t = \left(\frac{\pi}{U^n 2^n \mathrm{B}((n+1)/2,(n+1)/2)}\right)^{1/(n-m)};$$

- for $m = n$, this happens at $t = 0$ when

$$U = \frac{\pi}{2^n \mathrm{B}((n+1)/2,(n+1)/2)},$$

  with the solution valid for all time for U less than this critical value, and the behaviour unclear for U larger than this critical value;

- for $m > n$, this happens at $t = 0$ for all $U > 0$.

We can again relate this to the pressure. Upon evaluating (2) on the impactor, a simple asymptotic expansion near the trailing turnover

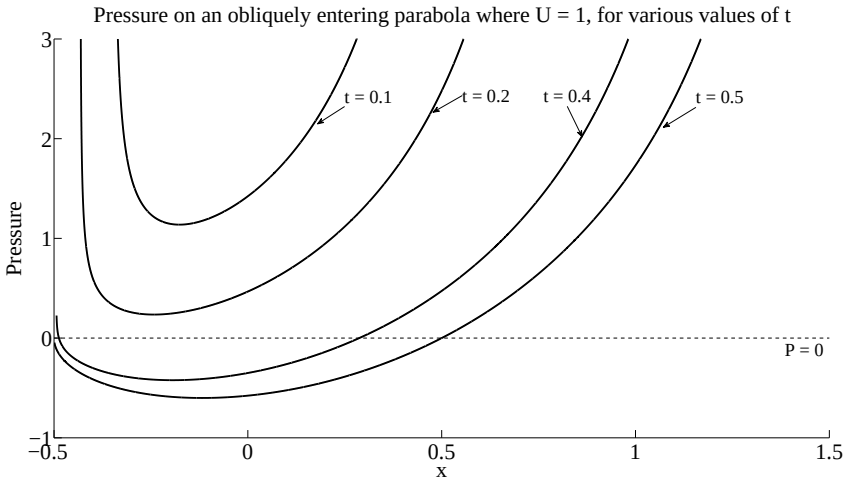

Figure 4. The pressure on a parabolic impactor for various times with $U = 1$. The critical time at which the trailing turnover point stops advancing is given by $t = 1/2$. It is clear that the pressure vanishes at $d_- = -1/2$ when t reaches this critical value. At times $t = 0.1, 0.2, 0.4, 0.5$ respectively the pressure minimum is at $x = -0.1764, -0.2423, -0.1937, -0.1181$, with value $p = 1.1377, 0.2359, -0.4222, -0.6006$.

point, $Ut - d(t)$, allows us to find the coefficient of the inverse square-root singularity in the pressure near there. We find that

$$p \sim \frac{A(t)}{\sqrt{x - (Ut - d(t))}} \quad \text{as} \quad x \to Ut - d(t),$$

where

$$A(t) = \frac{\sqrt{d(t)}}{\sqrt{2}\pi}(U - \dot{d}(t))^2 \times \lim_{\gamma \to 0} \left[\int_{-d+\gamma}^{d} \frac{1}{(\xi + d)^{3/2}} \frac{s(t) - f(\xi)}{\sqrt{d - \xi}} \mathrm{d}\xi - \left(\frac{s(t) - f(-d)}{\sqrt{d}} \right) \sqrt{\frac{2}{\gamma}} \right], \quad (6)$$

so that the coefficient of the inverse square-root singularity vanishes as the speed of that turnover point tends to zero. This is consistent with the wedge example we described previously.

The case $m = 1, n = 2$ is displayed in Figure 4. In this case, $d_\pm = Ut \pm \sqrt{2t}$ and the critical time at which the trailing turnover point stops advancing is $t = 1/(2U^2)$. Prior to breakdown, we can clearly see a region of negative pressure forming on the impactor, particularly on the trailing side. This region grows in size as we approach the critical time, and the trailing point of zero pressure coincides with the trailing

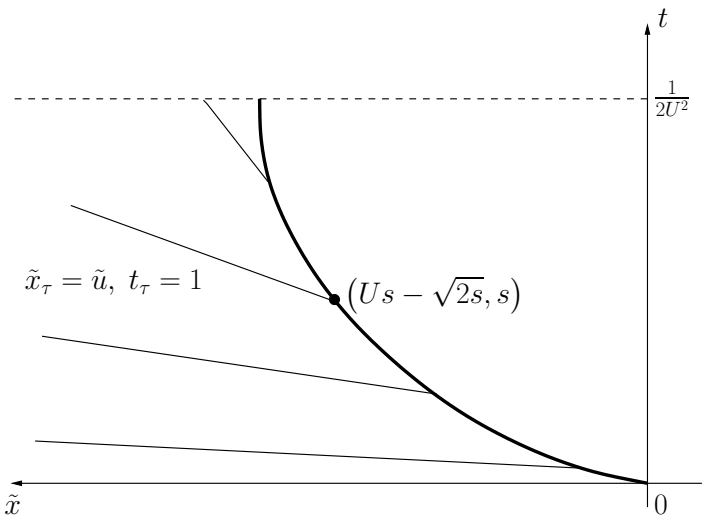

Figure 5. Characteristic diagram of the leading-order trailing splash jet problem for the constant-speed oblique impact of a parabola. The bold curve is the turnover curve, $\tilde{x} = d(t)$. We parametrise the boundary data, as given by (5), by s on this curve. The straight lines are the characteristics, along which time-of-travel is parametrised by τ, depicted emanating from this curve. Note that as we approach the critical time, depicted by the dashed line, the slope of the characteristics becomes unbounded.

turnover point at $t = 1/(2U^2)$, with the inverse square-root singularity vanishing.

As in the case of wedge impact, we have the possibility of cavitation occurring on the impactor prior to breakdown due to this region of negative pressure.

Considering the example of the parabola, it is simple to solve the zero-gravity shallow-water equations governing the jet problem using the method of characteristics. We parametrise along a characteristic by τ and parametrise the boundary data on the turnover curve given by (5) by $s \in \left(0, 1/2U^2\right)$. Breakdown corresponds to $s \to 1/(2U^2)$. If, in local coordinates moving with the body, we denote the distance along the body by $\tilde{x}$ and the corresponding component of velocity in the $\tilde{x}$-direction by $\tilde{u}$, it is trivial to note that the leading-order characteristics are particle paths, as shown in, for example, [9]. We depict the characteristic diagram in Figure 5. We note that

$$\frac{\partial \tilde{x}}{\partial \tau} = \tilde{u} = 2\left(U - \frac{1}{\sqrt{2s}}\right) \to 0 \quad \text{as} \quad s \to \frac{1}{2U^2},$$

so that no information is carried into the jet at breakdown, as was the case with the wedge impact. Equivalently, there is no flow of fluid into the jet at this time, although the thickness of the jet at the turnover curve remains finite. It can be shown that this form of breakdown in the trailing splash jet extends to more general profiles where $m < n$.

5. Summary

Having corrected an apparently minor error in [7], we discussed the solution and breakdown of Wagner theory for two-dimensional oblique impact problems. In particular, the absence of any time dependence in the displacement potential formulation of the leading-order outer problem enabled us to transform the oblique impact problem to the corresponding normal impact problem. We were thus able to show that the leading-order turnover points and leading-order outer free surface are readily determined from their normal impact counterparts. In the particular example of a symmetric body profile, the turnover points and free surface are symmetric about the minimum of the impactor to leading-order. There is no symmetry, however, in the leading-order outer velocity potential or pressure.

Our model for oblique impacts breaks down at the first instant that one of the turnover points stops advancing. This breakdown is characterised in several ways:

- The local-in-space-and-time linear stability analysis of [8] dictates that the problem is no longer stable to out-of-plane perturbations when the turnover point is not advancing.

- Solving the hyperbolic problem for the leading-order outer free surface is no longer possible as we lose causality; the characteristics are exiting the turnover curve rather than entering it. Thus we cannot determine the width of the equivalent flat plate in Wagner theory and hence the location of the turnover points.

- The coefficients of the inverse-square root singularities in the expansions of the leading-order outer pressure on the impactor and leading-order outer velocity at the trailing turnover point vanish at breakdown.

- The solution to the zero-gravity shallow water equations in the splash jet problem becomes invalid as the characteristics are parallel to the boundary curve.

We finally noted that, in both the oblique impact of a wedge and of a parabola, regions of negative pressure form on the impactor prior to breakdown. These regions grow in size as we approach breakdown, with the trailing points of zero pressure coinciding with the trailing turnover point at breakdown. Hence, it is possible that a patch cavity, as modelled in [6], forms on the impactor due to this negative pressure.

The ideas outlined in this paper extend to three-dimensional oblique impact problems. Work on this is currently ongoing, and will be reported elsewhere.

Acknowledgements

The authors wish to thank the reviewers for some helpful comments. This publication was based on work supported in part by Award No. KUK-C1-013-04, made by King Abdullah University of Science and Technology (KAUST). M.R.M. would like to acknowledge the ESPRC for financial support via a studentship. J.R.O. was in receipt of a Leverhulme Emeritus Fellowship.

References

1. Chekin, B.S. (1989) The entry of a wedge into an incompressible fluid. J. Appl. Math. Mech. 53(3):300–307
2. Garabedian, P.R. (1953) Oblique water entry of a wedge. Comm. Pure Appl. Math. 6(2):157–165
3. Judge, C. and Troesch, A. and Perlin, M. (2004) Initial water impact of a wedge at vertical and oblique angles. J. Eng. Math. 48(3):279–303
4. Korobkin, A.A. (1988) Inclined entry of a blunt profile into an ideal fluid. Fluid Dynamics 23(3):443–447
5. Korobkin, A.A. (2003) Cavitation in liquid impact problems. In: Proceedings of the Fifth International Symposium on Cavitation, Osaka, 1–4 November 2003
6. Howison, S.D., Morgan, J.D. and Ockendon, J.R (1994) Patch cavitation in flow past a rigid body. In: Blake, J.R., Boulton-Stone, J.M. and Thomas, N.H. (eds) Proceedings IUTAM Symposium on Bubble Dynamics and Interface Phenomena 23:219–226, Kluwer, Dordrecht
7. Howison, S.D., Ockendon, J.R. and Oliver, J.M. (2004) Oblique slamming, planing and skimming. J. Eng. Math. 48:321–337
8. Howison, S.D., Ockendon, J.R. and Wilson, S.K. (1991) Incompressible water-entry problems at small deadrise angles. J. Fluid Mech. 222:215–230
9. Oliver, J.M. (2002) Water entry and related problems. DPhil Thesis, University of Oxford
10. Semenov, Y.A. and Yoon, B.S. (2009) Onset of flow separation for the oblique water impact of a wedge. Phys. Fluids 21:112103–11
11. Wagner, H. (1932) Über Stoß- und Gleitvorgänge an der Oberfläche von Flüssigkeiten. Z. angew. Math. Mech. 12:193–215